BJRS

BRAZILIAN JOURNAL
OF
RADIATION SCIENCES
10-02 (2022) 01-10

Synthesis of Thulium-yttria Nanoparticles with EPR Response

Santos[a] S.C., Rodrigues[b] O.Jr., Campos[c] L.L.

[a-c] *Instituto de Pesquisas Energéticas e Nucleares IPEN\CNEN-SP /Center of Radiation Metrology, 05508-000, São Paulo, São Paulo, Brazil*

silas.cardoso@alumni.usp.br

ABSTRACT

Approaches to form new materials for radiation dosimetry are essential to enhance quality assurance and quality improvement practices based on radiation protection concept. The present work reports a hydrothermal synthesis based on a relative low temperature and pressure to form thulium-yttria nanoparticles with electron paramagnetic resonance response. Thulium-yttria nanoparticles were prepared and characterized by XRD, SEM, PCS, and EPR. According to results, the hydrothermal method provided thulium-yttria nanoparticles with cubic C-type structure, mean particle size (d_{50}) less than 160nm, and EPR response. The EPR spectra of powders exhibited two resonance peaks p1 and p2 recorded at 350 and 160mT, respectively. The enhancement of the EPR response of yttria by the use of thulium as a dopant provide meaningful parameters to advance in the formation of new rare earth-based materials for radiation dosimetry.

Keywords: **yttria, thulium oxide, EPR, radiation dosimetry, ceramic processing.**

ISSN: 2319-0612
DOI: https://10.15392/bjrs.v10i2A.1801
Submitted:2021-12-24
Accepted: 2022-03-23

1. INTRODUCTION

The design and formation of new materials for radiation dosimetry are essential to improve practices where ionizing radiation is used [1-3]. The hydrothermal synthesis [4] offers the possibility to build up smart structures from colloidal suspensions, whereby the formation of particles is based on controlled chemical stoichiometry. Innovative contributions using this method have been reported elsewhere [5]–[10].

The rare earths (RE) exhibit unique chemical and physical properties, being addressed as critical materials by The European Union and United States of America.[11], [12] Belong to the RE group, yttria (Y_2O_3) has been used as a host material of other REs due to its intrinsic lattice characteristics that enable the insertion of other RE ions into its structure (doping), providing the development of advanced structures and useful applications in transparent ceramics[13], lasers[14], biomaterials[15], and energy[16]. Oliveira et al. [17] obtained multi-colour-emitting, high-crystalline and micro-sized Y_2O_3:Eu^{3+},Er^{3+},Yb^{3+} particles using sorbitol as an alternative to enhance the luminescence of Pechini-derived phosphors. In our recent study [18], it was found out that the dosimetric characteristics of yttria were improved by using 2at.%Eu as dopant. A linear EPR dose-response behaviour was recorded in a range of dose from 0.001 to 50kGy.

The effect of thulium (Tm) as dopant/activator of ceramic/glasses materials has been reported elsewhere [19]–[21]. The motivation of selecting Tm as dopant of yttria consists in the fact that the electronic levels of Tm ions can interact with the energy levels of yttria, and an improvement of yttria characteristics for radiation dosimetry may be achieved.

The present paper reports the formation of thulium-yttria nanoparticles with controlled particle characteristics and EPR response by an alternative hydrothermal synthesis. The results suggest that the thulium-yttria nanoparticles are promising materials for radiation dosimetry.

2. MATERIALS AND METHODS

Thulium-yttria powders (Y_2O_3:Tm) with controlled characteristics such as stoichiometry, shape, size, and density were synthesized using the following starting materials: yttria (Y_2O_3, 99.99%, Alfa

Aesar GmbH), thulium oxide (Tm_2O_3, 99.999%, Alfa Aesar GmbH), nitric acid (HNO_3, Synth), ammonium hydroxide (NH_4OH, Casa Americana).

A facile hydrothermal process [22] was performed to synthesize Y_2O_3:Tm powders, with thulium content varying from 0.1 up to 2.0at% (at.%, atomic percentage). All powder compositions were formed by stoichiometry calculations considering yttria and thulium oxide. The precursor powders were obtained from a stock solution processed at 60ºC for 6h in a condenser system.

The as synthesized Y_2O_3:Tm powders were characterized as follows: mean particle size (d_{50}) by Photon Correlation Spectroscopy (PCS, Litesizer500, Anton Paars), using hydrodynamic diameter model [23]X-ray diffraction (XRD, Rigaku Multiflex, Japan), with an angular range (2θ) from 15 to 70º, scanning of $0.5^{o}.min^{-1}$ and Kα source, in which the crystallite size was calculated by Scherrer model[24], and based on the measurement of full-width at half-maximum (FWHM) values in the corresponding XRD pattern; helium pycnometry (Pycnometer Micrometrics 1330), and Scanning Electron Microscopy (SEM, INC Ax-act, Oxford Instruments).

The paramagnetic response of Y_2O_3:Tm powders as a function of dopant concentration (Tm^{3+}) was evaluated by electron paramagnetic resonance using an X-band EPR spectrometer (Bruker EMX PLUS), under room temperature and atmosphere. EPR spectra of samples were recorded in field modulation frequency of 100kHz, microwave power of 2.5mW, center field of 300mT, sweep width of 300mT, modulation amplitude of 0.4mT, time constant of 0.01ms, 10 scans, temperature of 20ºC, environmental atmosphere, at controlled humidity, and using DPPH (2,2-Diphenyl-1-picrylhydrazyl, Bruker) as EPR reference.

3. RESULTS AND DISCUSSION

XRD curves of thulium-yttria powders with up to 2at.%Tm are shown in Fig.1. Based on the results all samples exhibited cubic C-type structure, without secondary phases, corresponding to JCPDS 25-1200. The presence of thulium ions into yttria structure does not change considerably the lattice arrangement, because yttrium and thulium present similar ionic radius. Thus, the doping is characterized as substitutional, and no lattice distortion is induced. These results reveal that the hydrothermal synthesis successfully produced thulium-yttria powders with controlled crystalline structure.

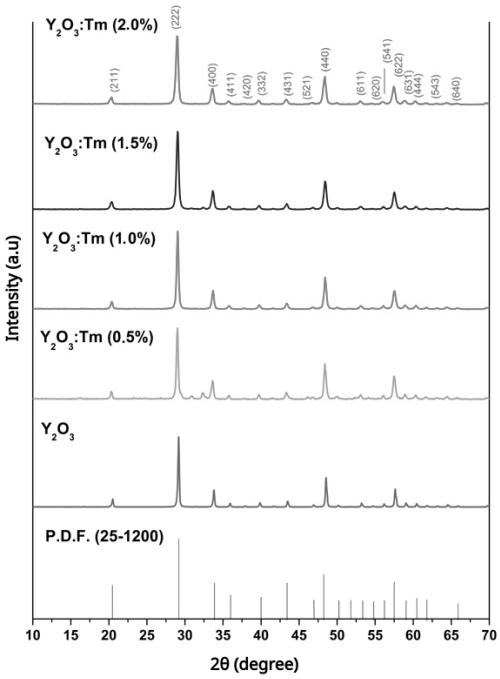

Figure 1. XRD curves of Y_2O_3:Tm powders synthesized by hydrothermal synthesis, followed by thermal treatment at 1100ºC for 2h in room atmosphere.

Particle characteristics of thulium-yttria powders up to 2at.%Tm are illustrated in Fig.2. The variation of the mean particle size (d_{50}) as a function of Tm content is illustrated in Fig.2a. According to results the increase of Tm content provided an increase of the mean particle from 50 to 150nm. Besides, SEM image illustrated in Fig. 2b revealed that thulium-yttria powders (0.5at% Tm) are constituted by fine particles, with rounded morphology and size smaller than 1µm. Moreover, crystallite size (d_c) represented in Fig. 2c exhibited a small variation (between 5 and 6.8nm), which confirms the "substitution characteristic" of doping. The control of particle characteristics contributes directly with the whole ceramic processing as dispersion, shaping, and sintering. By this way, ceramic bodies with smart end-use can be formed. . On the other hand, the pycnometric density (Fig.2d) increased significantly from 4.6 ("pure yttria", 0at.%Tm) to 5.8g.cm^{-3} (2at.% Tm)

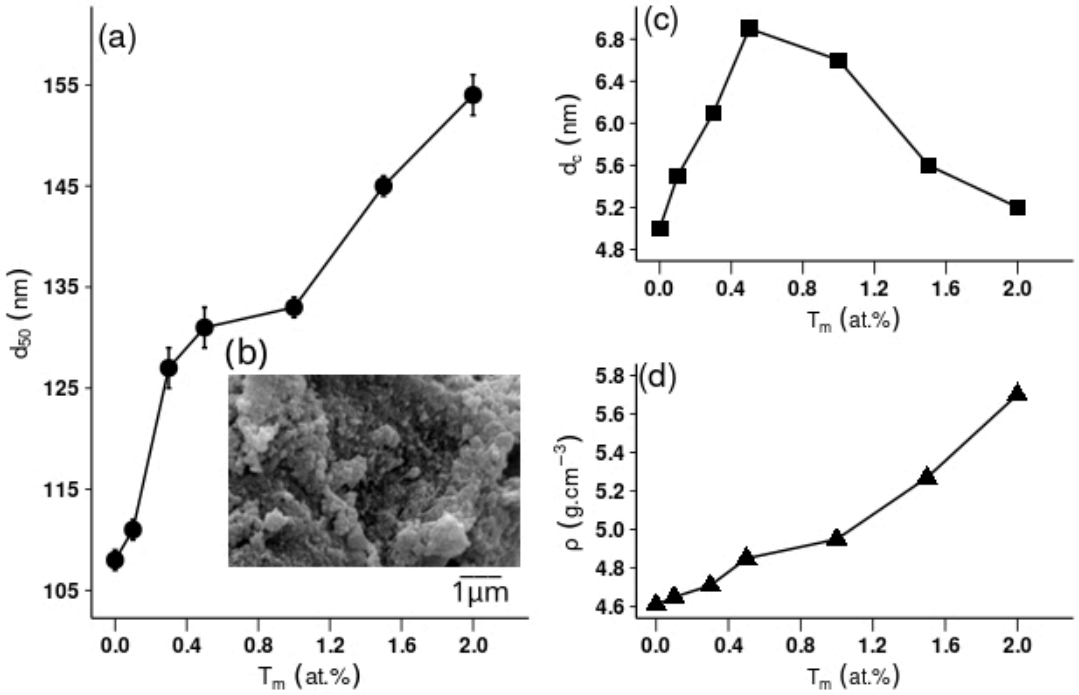

Figure 2. Thulium-yttria powder characteristics: (a) mean particle size (d_{50}); (b) SEM image of composition prepared with 0.5at.%Tm; (c) crystallite size (dc); and (d) pycnometric density (ρ).

Processing steps as synthesis, washing, grinding, as well as radiation provide the development of unpaired electrons in materials. The Electron Paramagnetic Resonance (EPR) is a non-destructive and non-intrusive technique that provides structural information from chemical and physical processes by detection of unpaired electrons [25]. Thus, EPR is a useful technique to advance in development of rare earth-based dosimetry materials.

The EPR spectra of thulium-yttria powders prepared with up to 2at.%Tm are illustrated in Fig.3. The major peak p1 is associated to interstitial ion O^{2-} from adsorption of oxygen from atmosphere [26], and was recorded at 350mT, with a width of 3mT, and g-value 2.0040. Based on yttria spectra, a shift around of 0.0040 on g-value was observed. The addition of Tm^{3+} led the formation of an additional resonance peak p2, which is associated to F^{+} center i.e oxygen vacancies containing a remaining electron, recorded at 164.0mT and g-value 2.0065. Moreover, the p1 peak exhibited remarkable increase for composition 1.5at% Tm compared with "pure" yttria powders.

The insertion of low concentrations of Tm provided substantial formation of crystal defects, which in turn can trap more unpaired electrons formed during materials processing, including

irradiation. In addition, the best results observed for the samples prepared with 1.5%Tm can be explained considering the crystalline features of yttria. According to Zych et al. [27], the solid-state behavior of yttria is associated with the symmetry axis where the RE ions (dopant) are located. As RE ion are located at C_{3i}, S_6 symmetry axes, few electron transitions occur and the luminescence response is low. On the other hand, as RE ions fill C_2 symmetry, transitions $^5D_0$ - $^7F_2$ occur and the luminescence response is high.

Based on the results, doping yttria with thulium enhances the EPR response of samples due to the formation of new defects, as well as energy transfer from Tm^{3+} ion to yttria host.

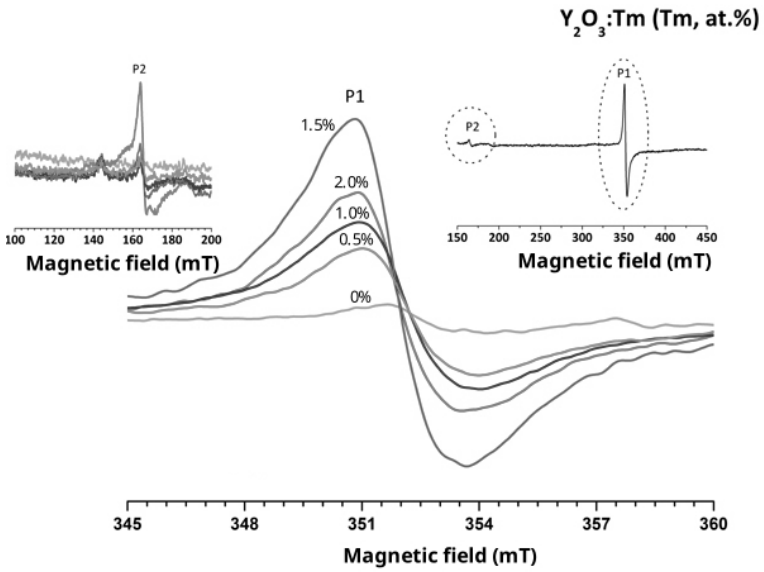

Figure 3. EPR curves of as synthesized powders of thulium-yttria recorded in environmental temperature.

4. CONCLUSIONS

Cubic C-type thulium-yttria nanoparticles with mean particle size less than 160nm, and electron paramagnetic resonance (EPR) response were obtained by hydrothermal synthesis, followed by thermal treatment at 1100°C for 2h in environmental atmosphere. Among all compositions evaluated, thulium-yttria nanoparticles prepared with 1.5at.%Tm presented the most intense EPR

response. The present synthesis was successful to produce rare-earth nanoparticles with promising characteristics for radiation dosimetry.

ACKNOWLEDGMENT

The authors are very grateful to Dr. Maria Elisa Chuery Martins Rostelato of the Radiation Technology Center (CTR) at the Nuclear and Energy Research Institute who kindly allowed us to use the zeta potential analyzer, and Dr. Beatriz Ribeiro Nogueira MSc at the same center who helped us with our first use of the equipment. In addition, we acknowledge the following sponsor organizations: São Paulo Research Foundation (FAPESP), National Council for Scientific and Technological Development (CNPq), and Coordination for Improvement of High Degree People (CAPES).

REFERENCES

[1] *Occupational Radiation Protection*, no. GSG-7. Vienna: INTERNATIONAL ATOMIC ENERGY AGENCY, 2018.

[2] *Radiation Protection of the Public and the Environment*, no. GSG-8. Vienna: INTERNATIONAL ATOMIC ENERGY AGENCY, 2018.

[3] *Radiation Protection and Safety of Radiation Sources: International Basic Safety Standards*, no. GSR Part 3. Vienna: INTERNATIONAL ATOMIC ENERGY AGENCY, 2014.

[4] E. Suvaci and E. B. T.-R. M. in M. S. and M. E. Özel, "Hydrothermal Synthesis," Elsevier, 2020.

[5] M. S. Medina, J. C. Bernardi, A. Zenatti, and M. T. Escote, "A new approach to obtain calcium cobalt oxide by microwave-assisted hydrothermal synthesis," *Ceram. Int.*, vol. 46, no. 2, pp. 1596–1600, 2020, doi: https://doi.org/10.1016/j.ceramint.2019.09.130.

[6] X. Yu, Z. Han, H. Tang, J. Xie, and X. Mi, "Investigating luminescence properties and energy transfer of Ca3(PO4)2: Dy3+/Eu3+ phosphor via hydrothermal synthesis," *Opt. Mater. (Amst).*, vol. 106, p. 110009, 2020, doi: https://doi.org/10.1016/j.optmat.2020.110009.

[7] S. H. Daryan, A. Khavandi, and J. Javadpour, "Surface engineered hollow hydroxyapatite microspheres: Hydrothermal synthesis and growth mechanisms," *Solid State Sci.*, vol. 106, p. 106301, 2020, doi: https://doi.org/10.1016/j.solidstatesciences.2020.106301.

[8] M. L. Hancock *et al.*, "The characterization of purified citrate-coated cerium oxide nanoparticles prepared via hydrothermal synthesis," *Appl. Surf. Sci.*, vol. 535, p. 147681, 2021, doi: https://doi.org/10.1016/j.apsusc.2020.147681.

[9] H. Wu *et al.*, "Cellulose nanofiber assisted hydrothermal synthesis of Ni-rich cathode materials with high binding particles for lithium-ion batteries," *J. Alloys Compd.*, vol. 829, p. 154571, 2020, doi: https://doi.org/10.1016/j.jallcom.2020.154571.

[10] N. J. Ismail *et al.*, "Hydrothermal synthesis of TiO2 nanoflower deposited on bauxite hollow fibre membrane for boosting photocatalysis of bisphenol A," *J. Water Process Eng.*, vol. 37, p. 101504, Oct. 2020, doi: 10.1016/j.jwpe.2020.101504.

[11] U. S. G. S. Department of the Interior, U. S. G. S. Department of the Interior, and U. S. G. S. Department of the Interior, "A Federal Strategy to Ensure Secure and Reliable Supplies of Critical Minerals," United States, 2018. [Online]. Available: https://www.usgs.gov/news/interior-releases-2018-s-final-list-35-minerals-deemed-critical-us-national-security-and.

[12] T. E. Union and O. of the E. Union, "Report on critical raw materials and the circular economy ," The European Union, 2018. doi: 10.2873/167813.

[13] S. Khalili, A. Nourmohammadi, and M. Milani, "Influence of process parameters in gel casting of a pure yttria nanopowder to fabricate transparent ceramics," *Ceram. Int.*, vol. 47, no. 21, pp. 29977–29987, 2021, doi: https://doi.org/10.1016/j.ceramint.2021.07.172.

[14] Y.-S. Kim, Y.-R. Lee, B.-J. Kim, J.-H. Lee, S.-H. Moon, and H. Lee, "Characterization of amorphous yttria layers deposited by aqueous solutions of Y-chelate alkoxides complex," *Phys. C Supercond. its Appl.*, vol. 508, pp. 42–48, 2015, doi: https://doi.org/10.1016/j.physc.2014.10.013.

[15] H. Reveron and J. Chevalier, "Yttria-Stabilized Zirconia as a Biomaterial: From Orthopedic Towards Dental Applications," M. B. T.-E. of M. T. C. and G. Pomeroy, Ed. Oxford: Elsevier, 2021, pp. 540–552.

[16] N. M. El-Shafai, M. S. Ramadan, M. A. Amin, and I. M. El-Mehasseb, "Graphene oxide/cellulose derivative nanohybrid membrane with Yttrium oxide: Upgrading the optical and electrochemical properties for removing organic pollutants and supercapacitors

implementations," *J. Energy Storage*, vol. 44, p. 103344, 2021, doi: https://doi.org/10.1016/j.est.2021.103344.

[17] N. A. Oliveira, A. G. Bispo-Jr, G. M. M. Shinohara, S. A. M. Lima, and A. M. Pires, "The influence of the complexing agent on the luminescence of multicolor-emitting Y2O3:Eu3+,Er3+,Yb3+ phosphors obtained by the Pechini's method," *Mater. Chem. Phys.*, vol. 257, p. 123840, Jan. 2021, doi: 10.1016/j.matchemphys.2020.123840.

[18] S. C. Santos, O. Rodrigues, and L. L. Campos, "EPR response of yttria micro rods activated by europium," *J. Alloys Compd.*, Jun. 2018, doi: 10.1016/j.jallcom.2018.06.063.

[19] N. L. Wang, X. Y. Zhang, and Z. H. Bai, "Synthesis of neodymium doped yttria nanopowders by microwave-assisted glycine combustion method and the powder characteristics," *Ceram. Int.*, vol. 40, no. 3, pp. 4903–4908, 2014, doi: DOI 10.1016/j.ceramint.2013.10.073.

[20] H. K. Jung *et al.*, "Luminescent and magnetic properties of cerium-doped yttrium aluminum garnet and yttrium iron garnet composites," *Ceram. Int.*, vol. 45, no. 8, pp. 9846–9851, 2019, doi: https://doi.org/10.1016/j.ceramint.2019.02.023.

[21] E. F. Huerta, J. De Anda, I. Martínez-Merlin, U. Caldiño, and C. Falcony, "Near-infrared luminescence spectroscopy in yttrium oxide phosphor activated with Er3+, Li+ and Yb3+ ions for application in photovoltaic systems," *J. Lumin.*, vol. 224, p. 117271, 2020, doi: https://doi.org/10.1016/j.jlumin.2020.117271.

[22] S. C. Santos, O. Rodrigues, and L. L. Campos, "Colloidal processing of thulium-yttria microceramics," *J. Phys. Chem. Solids*, vol. 161, p. 110420, 2022, doi: https://doi.org/10.1016/j.jpcs.2021.110420.

[23] W. Tscharnuter, *Photon Correlation Spectroscopy in Particle Sizing*, 1st ed. United States of America: John Wiley & Sons Ltd, 2000.

[24] A. L. Patterson, "The Scherrer Formula for X-Ray Particle Size Determination," *Phys. Rev.*, vol. 56, no. 10, pp. 978–982, Nov. 1939, doi: 10.1103/PhysRev.56.978.

[25] G. R. Eaton and S. S. Eaton, "2.03 - Electron Paramagnetic Resonance Spectroscopy," E. C. Constable, G. Parkin, and L. B. T.-C. C. C. I. I. I. Que Jr, Eds. Oxford: Elsevier, 2021, pp. 44–59.

[26] J. H. Lunsford, "Esr of Adsorbed Oxygen Species," *Catal. Rev. Eng.*, vol. 8, no. 1, pp. 135–157, 1973.

[27] E. Zych, M. Karbowiak, K. Domagala, and S. Hubert, “Analysis of Eu3+ emission from different sites in Lu2O3,” *J. Alloys Compd.*, vol. 341, no. 1–2, pp. 381–384, 2002, doi: Pii S0925-8388(02)00042-7Doi 10.1016/S0925-8388(02)00042-7.